

BASEMENT STRUCTURES IN SANTOS BASIN (BRAZIL) FROM SATELLITE ALTIMETRY AND MARINE GEOPHYSICS

Renata Constantino¹ and Eder Cassola Molina²

ABSTRACT. This paper estimated the basement depth of the Santos Basin region, São Paulo State, Brazil, combining gravity data obtained from satellite altimetry and marine gravimetry, bathymetric data and sediment thickness from international data banks, and crustal thickness data available in the region. The first step consisted of calculating the gravity effect of sediments in Santos Basin, and the Crustal Mantle Interface (CMI) was modeled from constrained gravity inversion. Subsequently, the reliability of the models obtained was tested by flexural analysis with satisfactory results, as the flexural and gravimetric CMIs showed good agreement. The gravity effect of flexural CMI and the gravity effect of sediments were then calculated and subtracted from the original Bouguer anomaly. The residual field thus obtained, which is assumed to represent the topographical features of the basement, was inverted in the last step of the work, providing information that shows a basement with features of up to 700 m that appear to be in agreement with tectonic features previously discussed, such as the Avedis volcanic chain. The basement depth estimated during this study showed depths ranging from 1,500 to 10,500 m, and the deepest region is consistent with the Cabo Frio Fault. The methodology used in the study showed that from a combined data analysis, it is possible to obtain a three-dimensional model of the basement in ocean areas. This non-seismic approach can be advantageous in terms of efficiency and cost. The knowledge of the basement can offer important insights for the development of genetic and tectonic models of exploratory interest in the region.

Keywords: basement, Santos Basin, gravity.

RESUMO. Este trabalho visa estimar a profundidade do embasamento na região da Bacia de Santos por meio de uma análise combinada de dados gravimétricos obtidos a partir de altimetria por satélite e gravimetria marinha, com dados batimétricos e modelos de espessura sedimentar provenientes de bancos de dados internacionais e dados de espessura crustal disponíveis na região. Na primeira etapa do trabalho foi calculado o efeito do pacote sedimentar no sinal gravimétrico na Bacia de Santos, como também foi modelada a profundidade da Interface Crosta Manto (ICM) a partir de inversão gravimétrica com vínculos. Na etapa seguinte, a confiabilidade dos modelos obtidos foi testada através de análise flexural e o resultado foi satisfatório, mostrando que a ICM flexural e a ICM gravimétrica estão em concordância. Prosseguindo para etapa seguinte, o efeito gravimétrico da ICM encontrada por análise flexural e o efeito gravimétrico dos sedimentos foram então calculados e subtraídos da anomalia Bouguer original. O campo residual assim obtido, que se admite representar as feições topográficas do embasamento, foi invertido na última etapa do trabalho, fornecendo informações que mostram um embasamento com feições topográficas de até 700 m, que parecem estar em concordância com feições tectônicas discutidas em trabalhos pretéritos, como por exemplo a cadeia vulcânica Avedis. A profundidade do embasamento estimada durante este trabalho mostrou profundidades que vão desde 1.500 a 10.500 m, sendo que a região mais profunda corresponde à falha de Cabo Frio. Este trabalho demonstrou que, a partir de uma análise combinada de dados, é possível obter um modelo tridimensional do embasamento. O método, por ser não sísmico, pode ser vantajoso em questões de eficiência. O conhecimento deste embasamento é crucial na identificação de feições tectônicas, enquanto as informações sobre sua profundidade e topografia podem oferecer importantes subsídios para a elaboração de modelos genéticos e tectônicos de interesse exploratório na região.

Palavras-chave: embasamento, Bacia de Santos, gravimetria.

¹Universidade de São Paulo, Instituto de Geofísica, Astronomia e Ciências Atmosféricas, Geophysics Department, Room F101, Rua do Matão, 1226, 05508-090 São Paulo, SP, Brazil. Phone: +55(11) 3091-2791 – E-mail: renata@iag.usp.br

²Universidade de São Paulo, Instituto de Geofísica, Astronomia e Ciências Atmosféricas, Geophysics Department, Gravity and Geomagnetism Laboratory, Rua do Matão, 1226, 05508-090 São Paulo, SP, Brazil. Phone: +55(11) 3091-4755 – E-mail: eder@iag.usp.br

INTRODUCTION

The knowledge about the basement has great interest in geosciences because many of the geologic and tectonic processes of a given region are recorded on its surface. For geophysical studies aimed at investigating crustal structures, the topography of the basement is important because its features can be related to the spreading centers, ridges, trenches, tilted crustal blocks, and lineaments.

According to Braitenberg et al. (2006), the knowledge of the basement topography can be useful in several studies, such as determining the lateral density of lithosphere thickness variations through the principle of hydrostatic balance using the observed gravity field. In this case, it is necessary to calculate the crust load, which is determined by the depths of the basement and the ocean floor, the thickness of the crust and their respective densities (Ebbing et al., 2006).

Another application example can be found in data collection surveys carried out along profiles. Usually, these profiles are traced orthogonally to the lineaments. In cases where there is no basement topography data, bathymetric data are generally used, which can generate errors.

Obtaining data associated with the gravity field across satellite altimetry can be a good method for large-scale studies aimed at studying the crust because of their global distribution and good quality (Woodward & Wood, 2000).

In oceanic areas, the short wavelength component of the observed gravimetric signal is generally correlated with bathymetry. This has been used in past works such as by Smith & Sandwell (1997) and Sandwell & Smith (2001) to create bathymetry models from gravity field data.

Several studies are found in the literature where aspects of the ocean floor are investigated through satellite altimetry data. Smith & Sandwell (1997) used ship data together with satellite altimetry data to build a map of the topography of the oceans. Ramillien & Cazenave (1996) used *in situ* data obtained from the NGDC and ERS-1 GEODETIC MISSION data to globally calculate the bathymetry of the oceans. Calmant & Baudry (1996) showed different techniques for obtaining bathymetric models from satellite altimetry data.

In this work, the gravity data derived from altimetry satellites are used to map the basement topography. For this, the used gravity anomaly is corrected for the field generated by the sedimentary cover.

Between the water surface and the oceanic crust, there are three predominant density discontinuities:

- i) the water surface, marking the transition from air to water;

- ii) ocean floor, delimiting the transition from water to a solid material, usually sediment; and
- iii) basement, marking the transition from sediment to consolidated rock.

In the nomenclature used in this work, bathymetry corresponds to the ocean floor, and the basement irregularities correspond to the topography of the basement. The bathymetry of the ocean floor is usually obtained after hydrographic surveys. The ocean floor coincides with the basement topography only in regions where there is no sediment cover.

The interpretation of the gravity field related to the basement is of significant assistance in the interpretation of seismic data and in providing information in areas where such data are scarce or unavailable. This occurs in the Santos Basin, where, due to its high exploratory interest, much of the data collected and processed by companies in the energy sector are confidential.

This work aimed to determine the topography of the oceanic basement in the study region through the combined analysis of gravity anomaly data, bathymetric model, as well as the sediment thickness and crustal thickness models.

To this end, a number of specific objectives were achieved:

- i) modeling the CMI depth variations based on spectral analysis of observed gravity field;
- ii) modeling the CMI depth variations based on flexural deformation theory;
- iii) Isolating the observed gravity anomaly from the gravity signal of CMI and sediments, obtaining a residual gravity field; and
- iv) estimating the basement topography from the inversion of the residual gravity field thus obtained.

STUDY AREA

The Santos Basin is located in the southeastern region of the Brazilian continental margin between the 23°00'S and 28°00'S parallels, up to the bathymetric depth of 3,000 m. Its area has about 350,000 km², along the coastlines of Rio de Janeiro, São Paulo, Paraná and Santa Catarina (Moreira et al., 2007).

The Santos Basin is a passive margin basin whose origin is linked to the first tectonic pulses that caused the rupture of the Gondwana continent, in the Neocomian, resulting in the opening of the South Atlantic Ocean and separation of the African and American continents (Caldas & Zalán, 2009).

According to Mio et al. (2005), the Santos Basin resulted from the rifting processes during the African American separation, in

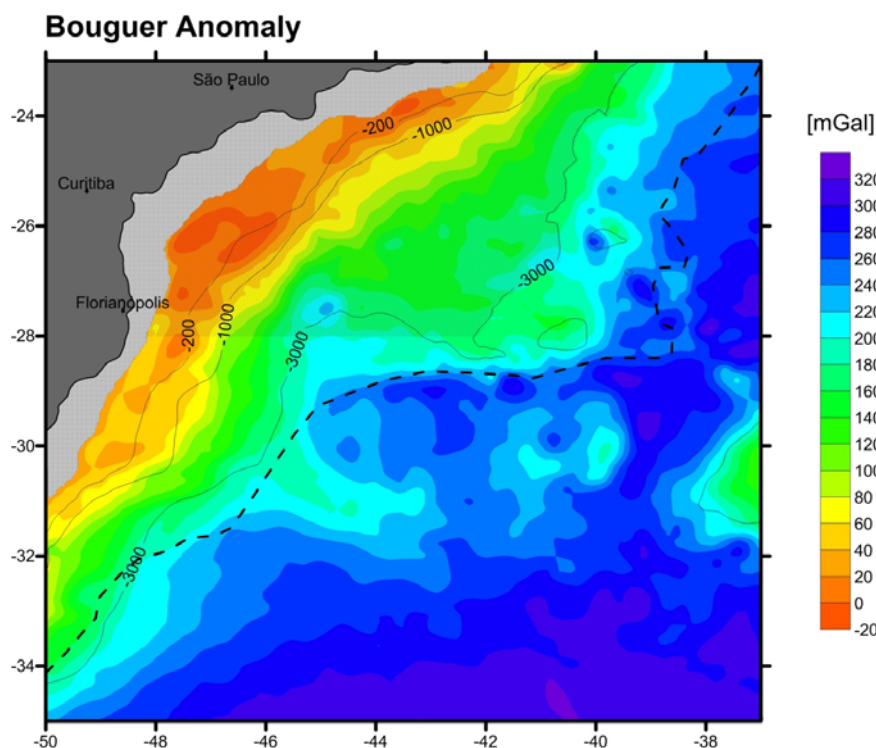


Figure 1 – Bouguer anomaly. The hatched regions (continuous and dotted lines) represent, respectively, the Santos Basin region, defined by Moreira et al. (2007) and the area where the gravity data are unreliable. The crustal limit, according to Cainelli & Mohriak (1999), is represented by the dashed line, and bathymetric contours refer to the depths 200, 1000 and 3000 m.

the Mesozoic. The accumulation of sediment occurred initially in fluvial-lacustrine conditions subsequently undergoing to an evaporite basin stage and evolving into a passive margin basin. These events are regarded as the basin's main evolutionary phases: rift, transition and passive margin.

According to these authors, the rift phase consists of a basal magmatism covered by a sequence deposited in fluvial-lacustrine environment, comprising shales, carbonates and thick alluvial fan deposits. The transition phase consists of a thick section of evaporitic rocks deposited during the Aptian in a restricted marine environment, with sabkha deposits. During the lower Albian, a wide carbonate platform, bordered by alluvial fan systems was installed over the transitional evaporite phase, starting the passive margin phase, that continues to the present.

The structural evolution of the basin is influenced by heterogeneities that affect both the crust and the mantle and comprise suture zones between the continental blocks, folding and thrust belts, shear zones and mafic dike swarms. These discontinuities controlled the structural framework of the basement of the Santos Basin through the reactivation of structures during the process of stretching and opening (Mio, 2005).

In this study, all data were processed for an area larger than the Santos Basin, due to two main factors: the lack of available seismic refraction data and better visualization of the results.

DATA SET

The methodology applied in this study the following data was needed: gravity, bathymetry sedimentary thickness and crustal thickness. The gravity data used are from Molina (2009), which are derived from several satellites geodetic missions and marine geophysics surveys in the South Atlantic region, from the U.S. National Geophysical Data Center and from the Brazilian EQUANT I and EQUANT II project cruises. Additional data from the LEP-LAC project were used to evaluate the model. Satellite altimetry data used are from the geodetic missions of ERS-1, GEOSAT, and SEASAT satellites. The model was developed with a spatial resolution of 2×2 arcmin and has an overall accuracy of 2.7 mGal for the free-air anomaly. Bouguer anomaly values are used in this study (Fig. 1).

The sedimentary thickness model (Fig. 2) was taken from the "Total Sediment Thickness of the World's Oceans and Marginal

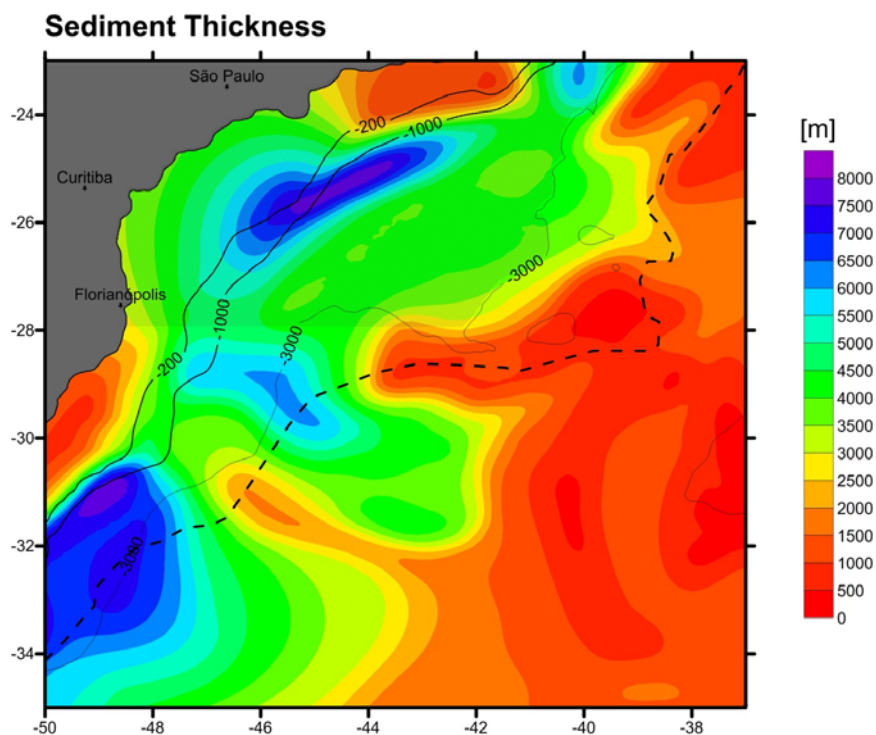


Figure 2 – Sediment thickness model obtained by NGDC. The hatched region is the Santos Basin area. The crustal boundary is represented by the dashed line, and the bathymetric contours refer to the depths 200, 1000 and 3000 m.

Seas, World Data Center for Marine Geology and Geophysics, Boulder” (Divins, 2003). The digital database of sedimentary thickness was compiled by the “National Geophysical Data Center” (NGDC) of National Oceanic and Atmospheric Administration (NOAA), with 5×5 arcmin resolution. Values, in meters, represent the depth the acoustic basement, defined as the deepest reflector observable in seismic reflection profiles, and may not represent the base of the sediments.

As this model has only information on the thickness of the sedimentary layer, additional data such as density and porosity were obtained from the Deep Sea Drilling Project (DSDP), site 356, from leg 39, located at 41.0880 S latitude and 28.2870 W longitude. This well was drilled down to 741 meters deep, and provide results from geochemical, geophysical and biological analyses. Further details can be found in Supko (1997).

The bathymetric data with 1 arcmin resolution are from GEBCO One Minute Grid (Fig. 3). The data are based on bathymetric contours of the GEBCO Digital Atlas-GDA (GEBCO, 2010), maintained by the British Oceanographic Data Centre (BODC) under the International Hydrographic Organization (IHO) and the Intergovernmental Oceanographic Commission (IOC) of UNESCO.

The crustal thickness data of Leyden et al. (1971) are from 33 refraction seismic profiles recorded along two lines between

Punta Del Este and Rio Grande, in June 1960. A total of 16 crustal thickness values were used.

Eleven additional values of crustal thickness were used from Zalán et al. (2011). These values resulted from the interpretation of 12,000 km of 2D seismic sections acquired by ION-GTX, coupled with gravimetry and magnetometry data and integrated with regional values available on the Petrobras database.

Gravity data, bathymetric data and the sedimentary thickness model were resampled to a grid at 4×4 km intervals to homogenize the geographical distribution of information.

METHODOLOGY

Data processing were carried out in four steps, based on the study developed by Braitenberg et al. (2006).

Step 1

The first step consists of modeling the CMI variations from the inversion of the gravity field.

The free-air anomaly data (Molina, 2009) were transformed into Bouguer anomaly using the classical formulation. Subsequently, the effect due to the sedimentary cover was removed from the resulting gravity field. The gravimetric effect of the sedimen-

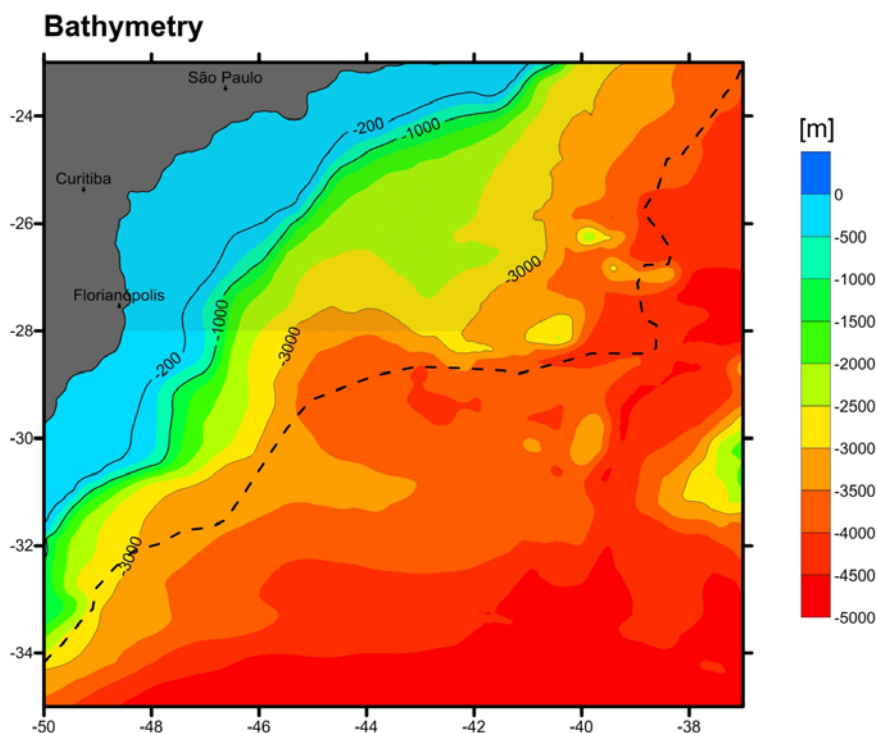


Figure 3 – Bathymetric data provided by GEBCO (2010). The hatched region is the Santos Basin area. The crustal boundary is represented by the dashed line, and the bathymetric contours refer to the depths 200, 1000 and 3000 m.

tary layer was calculated by the Parker algorithm (1972), which expands the gravity effect generated by the surface discontinuity into a fifth order series. The calculation can be performed with a constant density contrast for any discontinuity, however, for more realistic results, sediment compaction with depth should be considered. For this, we used the sediment compaction model described by Sclater & Christie (1980), based on an exponential reduction in porosity with depth. According to these authors, the density below the ocean floor (z) is calculated as:

$$\rho(z) = \rho_f \varphi_0 e^{-\frac{z}{d}} + \rho_g (1 - \varphi_0 e^{-\frac{z}{d}}) \quad (1)$$

where:

ρ_f = fluid density

ρ_g = grain/rock density

φ_0 = sediment initial porosity

d = decay parameter

z = depth

The gravity effect of sediment in the study area was calculated by applying this model to a series of thin layers (10 m thick), with variable lateral density.

The initial porosity and density values used are from the Deep Sea Drilling Project (DSDP) and correspond to 0.66 and

2750 kg/m³, respectively. The fluid density is standard, 1030 kg/m³ while the decay parameter was calibrated and set at 1.4 km.

After calculating the gravity effect of the sedimentary cover, the corrected field was inverted using the Iterative Constrained Inverse Modeling, described by Braitenberg & Zadro (1999).

Step 2

Step 2 involves the calculation of the equivalent topography based on Kumar et al. (2011), followed by the calculation of the flexure $w(\vec{r})$ using a flexure model for a thin plate (Turcotte & Schubert, 1982). For these calculations, it is necessary to know or estimate the flexural rigidity of the studied lithospheric plate. This step involves flexural analysis of the region, providing an independent means to determine the CMI undulations, allowing to test the reliability of the results of step 1. The flexural analysis is based on the methodology introduced by Braitenberg et al. (2002, 2003).

The thin plate flexure model predicts that the lithosphere responds to long-term (>1 Myr) loads, similarly to a thin elastic plate on a viscous fluid. In this study, the load is the sum of the intracrustal and topographic loads (referred to sediment).

This load has negative values because the water filled basins are less dense than the reference crust. According to Watts (2001) and Turcotte & Schubert (1982), the flexure $w(\vec{r})$, with $\vec{r} = (x, y)$, of a plate, loaded by the load $h(\vec{r})$, in the frequency domain, is defined as:

$$W(\vec{k}) = \frac{\rho_c}{\rho_m - \rho_c + \frac{D}{G} |\vec{k}|^4} H(\vec{k}) \quad (2)$$

where $W(\vec{k})$ is the Fourier transform (FT) of the plate flexure $w(\vec{r})$; $H(\vec{k})$, the FT topography; ρ_c , ρ_m the density of the crust and the mantle, respectively; g , the average gravity acceleration; $\vec{k} = k_x, k_y = 2\pi(v_x, v_y)$ the number of two-dimensional waves; v_x, v_y frequencies in space along the x - and y -axis, respectively. The parameter D is the flexural rigidity of the plate, which characterizes the lithosphere response to their loads (Karner & Watts, 1982) and is described by the equation

$$D = \frac{E T e^3}{12(1 - \sigma^2)} \quad (3)$$

where:

E = Young's modulus

σ = Poisson ratio

$T e$ = Effective elastic thickness

From the inverse Fourier transform of Eq. (2), the ratio between the two quantities is given in space by the relationship:

$$w(\vec{r}) = s(\vec{r}) * h(\vec{r}) \quad (4)$$

which describes the convolution of the load $h(\vec{r})$ with the flexural response of a point load $s(\vec{r})$. In the thin plate flexure model, it is generally admitted that the flexure $w(\vec{r})$ is approximately equal to the CMI leveling deviations.

For each node of the topographic load grid, one flexural response curve is calculated from the analytical solution (ASEP) described by Wienecke (2006). The flexure undulation of the corresponding CMI is obtained using a series of response functions to a point flexural load on convolution, each corresponding to a $T e$ value between 0-110 km, with 1-10 km intervals. Therefore, a set of flexural response curves was prepared, referring to $T e$ values between 0 and 25 km, with 1 km intervals. These values are based on Tassara et al. (2007).

To calculate the spatial variations of $T e$, the RMS error (root mean square) between the calculated CMI and the flexure CMI undulations can be determined in windows with side length L . The inverted $T e$ for a specific window is the one that minimizes the RMS error, and better fits the observed CMI.

The flexural rigidity was calculated using an average current window length of 100 km with a displacement of 20 km. The Young's modulus used was $E = 100$ GPa, the Poisson ratio $\sigma = 0.25$, and the gravity acceleration constant 9.81 m/s². The mantle bulk density (3370 kg/m³) and crust density (2880 kg/m³) are average values obtained from the density model CRUST 2.0.

Step 3

In this step, the CMI gravity effect is calculated with a constant density contrast along the discontinuity, applying the Parker algorithm (1972). The objective of this procedure is to remove from the observed gravity anomaly, the gravity signal of CMI and sediments:

$$g_{res} = g_{obs} - g_{CMI} - g_{sed} \quad (5)$$

The residual field thus obtained (g_{res}) is inverted in the next step of the methodology, providing the basement topography.

Step 4

The last step consists of inverting the residual gravity field (g_{res}) from the Iterative Constrained Inverse Modeling (Braitenberg & Zadro, 1999). This procedure was performed using the LITHO-FLEX software (Braitenberg et al., 2007).

RESULTS

The topography of the basement is calculated following the four steps outlined above.

The sediment layer contributes to the gravimetric signal with anomalies of -10 to -30 mGal. Figure 4 shows the corrected gravity field, without the signal of the sedimentary cover.

According to Blakely (1995), the long wavelength component is typically generated by the CMI undulations and the short-wavelength component from the surface masses. This fact does not mean that the surface masses do not contribute to the long wavelength portion of the wave, but the greatest contribution certainly is to the short wavelength. Thus, it is assumed that the CMI undulations are generated solely by the long wavelength.

To invert the data, the cutoff wavelength was estimated from the decay of the gravity field spectrum amplitude (Russo & Speed, 1994), and the value was found at 115 km.

The inversion process was performed for different contrast values of density and depth, which varied between 300-700 kg/m³ and 20-30 km, respectively. The same procedure was applied to variable lateral density contrast values, obtained from the CRUST 2.0, varying only the reference depth value.

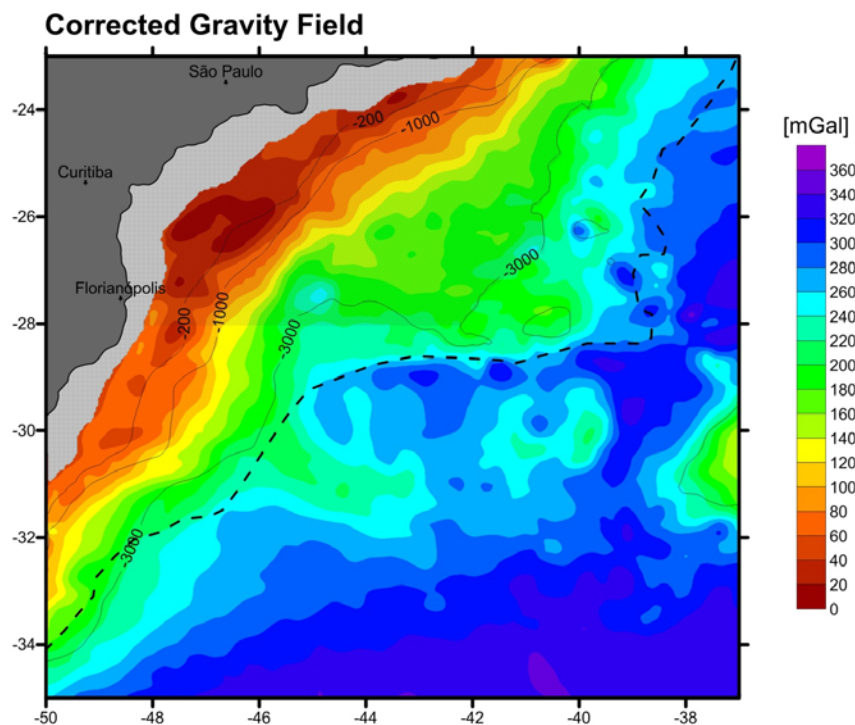


Figure 4 – Corrected gravity field, without the signal generated by the gravimetric sedimentary effect. The hatched regions (continuous and dotted lines) are, respectively, the area of the Santos Basin and the area where the gravity data are unreliable. The crustal boundary is represented by the dashed line, and the bathymetric contours refer to the depths 200, 1000 and 3000 m.

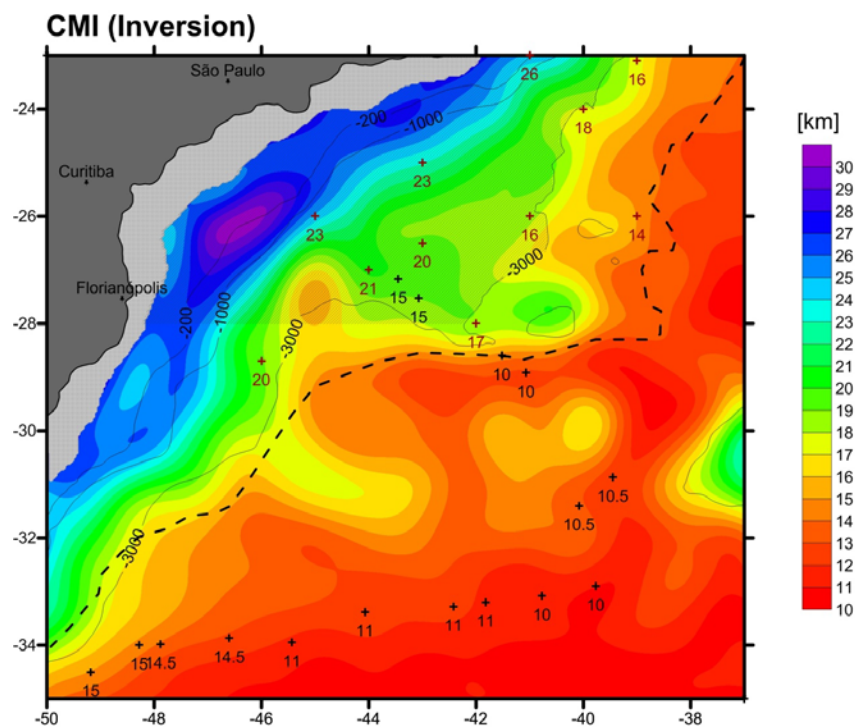


Figure 5 – Map of the Crust Mantle Interface (CMI) obtained from the inversion of the gravity field. The values in red are from Zalán et al. (2011) and values in black are from Leyden et al. (1971). The hatched regions (continuous and dotted lines) refer, respectively, to the Santos Basin area and the area where the gravity data are unreliable. The crustal boundary is represented by the dashed line, and the bathymetric contours refer to the depths 200, 1000 and 3000 m.

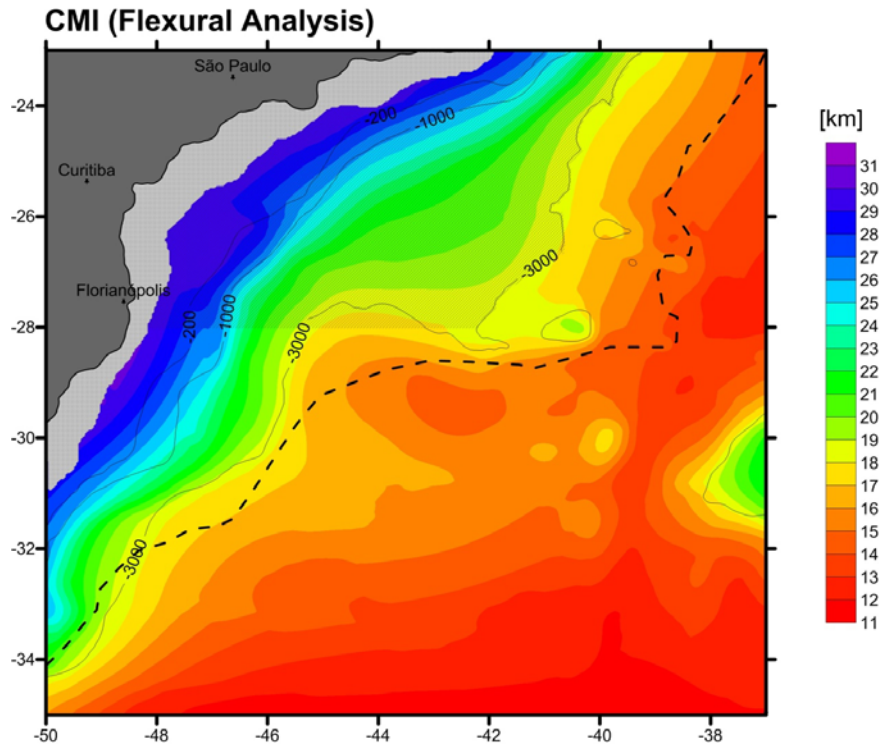


Figure 6 – Map of the Crust Mantle Interface (CMI) obtained from flexural analysis. The hatched regions (continuous and dotted lines) refer, respectively, to the Santos Basin area and the area where the gravity data are unreliable. The crustal boundary is represented by the dashed line, and the bathymetric contours refer to the depths 200, 1000 and 3000 m.

From these results, the RMS error was calculated between the data and some reference seismic values available. Some of these values, obtained from seismic refraction, are from Leyden et al. (1971). These values were not strictly located in the Santos Basin and, therefore, the study area had to be expanded. A second set of values, obtained from a combined analysis of seismic, gravity and magnetic data, are from Zalán et al. (2011).

The best result (Fig. 5), with the lowest RMS between the obtained values and constraints values, was calculated at 28.7 km deep, and for a laterally variable density contrast. The RMS error was approximately 1.9 km. Overall, the difference between the data obtained by the inversion of the gravity field and reference seismic values was small and less than 2 km at almost every point. Higher values are found only near the continental and oceanic crusts boundary.

Figure 6 shows the CMI calculated by flexural analysis. Note that the crustal thickness values range from 11 to 30 km. In the Santos Basin, the values near the coast are 30 km and reach 18 km close to the 3000 m bathymetric contour line.

Considering the area of the Santos Basin defined by Moreira et al. (2007), and assuming the oceanic continental crust bound-

ary defined by Cainelli & Mohriak (1999), the entire area of Santos Basin is located over continental crust, thus explaining the high crustal thickness values in the area.

At the continental and the oceanic crust boundary, the crustal thickness is approximately 16 km. The thinning of the oceanic crust reaches 11 km at the eastern end of the area (red). The crust is thicker in the proximity of the Rio Grande Rise approximately at coordinates 31 S, 37 W.

The flexural CMI values are in agreement with the gravity CMI, as seen in Figure 7, which shows the difference between the two CMIs. In general, the difference is small, ranging from 2.5 to 3 km. Positive values represent a shallower flexural CMI compared to the gravity CMI.

The highest values are close to the area where the results are not reliable (shaded in gray in the figure) and may represent, at least in part, the influence of such data.

The next step consisted of calculating the gravity effect of the CMI using the method of Parker (1972). The interface obtained by the flexural analysis was used for this calculation (Fig. 6).

After calculating the gravimetric signals produced by the sedimentary package and the CMI, both signals are subtracted

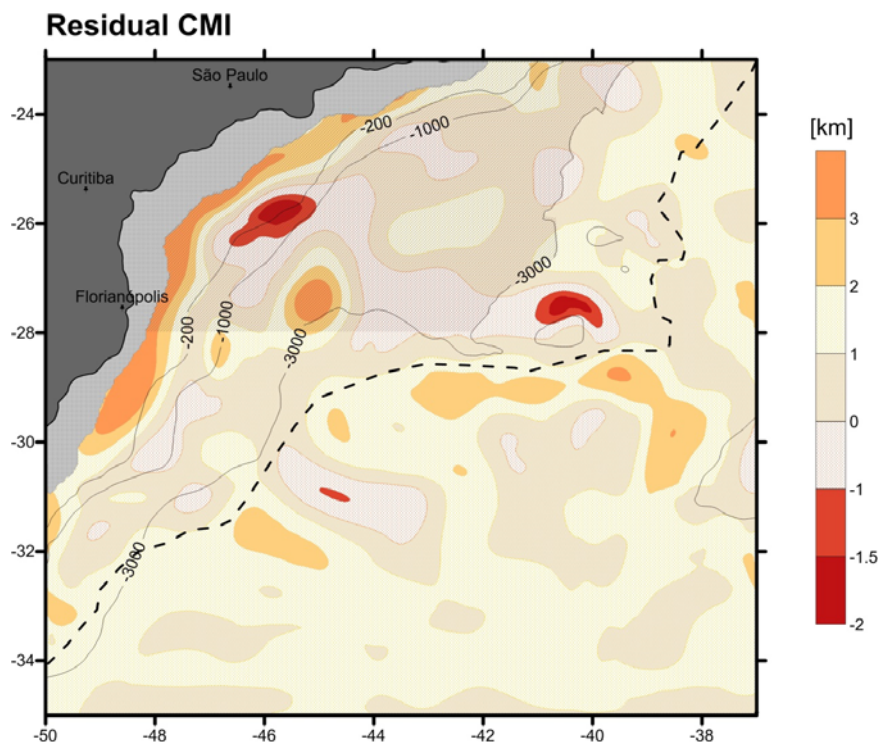


Figure 7 – The difference between depth values obtained by inversion of gravity field and flexural analysis. Positive values represent a flexural CMI shallower than the gravity CMI. The hatched regions (continuous and dotted lines) refer, respectively, to the Santos Basin area and the area where the gravity data are unreliable. The crustal boundary is represented by the dashed line, and the bathymetric contours refer to the depths 200, 1000 and 3000 m.

from the observed anomaly to obtain the residual field of the basement (Eq. 5). This field, called as residual gravity field (g_{res}), was inverted in the last step of this work.

A constant density contrast of 1570 kg/m^3 , referring to the contrast between the upper crust (2600 kg/m^3) and water (1030 kg/m^3), was used for inverting the residual field. The upper crust value was chosen using the data of the CRUST 2.0 model. During inversion, all wavelengths were considered. According to Hwang (1999), the inversion process can be done for a single reference depth that is defined as zero.

The term “basement” used in this work refers to the physical surface that lies below the sedimentary layer. The sedimentary thickness data represent the depth to the acoustic basement, defined as the deepest reflector observable in seismic reflection profiles and may not necessarily represent the sediment base. The end result corresponds to the base of the sediments and will be called “gravity basement” (Fig. 8).

Figure 8 shows the topography of the gravity basement, with depressions that are 700 m deep. In the Santos Basin area, the depth values vary considerably, ranging from 0 to 700 m.

Figure 9 shows the basement depth (the sum of bathymetry, sediment thickness) and gravity basement. Values range from 500 to 10,500 m. Inside the Santos Basin, lower values are observed close to the coast, north of the basin, and higher values of about 10,500 m are observed in the center, in red.

DISCUSSION

The comparison of the CMI model with the model input data, shows some residual values in the Santos Basin, especially residues between 10-20 mGal (Fig. 10). As only the portion of long wavelength was used during the inversion process, these values may be either reflecting the short wavelength present in the original data or the uncertainty of the calculated model.

One result of this work refers to the CMI undulations that obey the isostasy flexural theory and agree with the gravimetric CMI linked to seismic data.

The CMI undulations obtained by the flexural analysis compared to the gravimetric CMI, showed, in general, crustal thickness values ranging from 30 km to 11 km (Fig. 6). The difference between the two CMIs is shown in Figure 7. The negative values

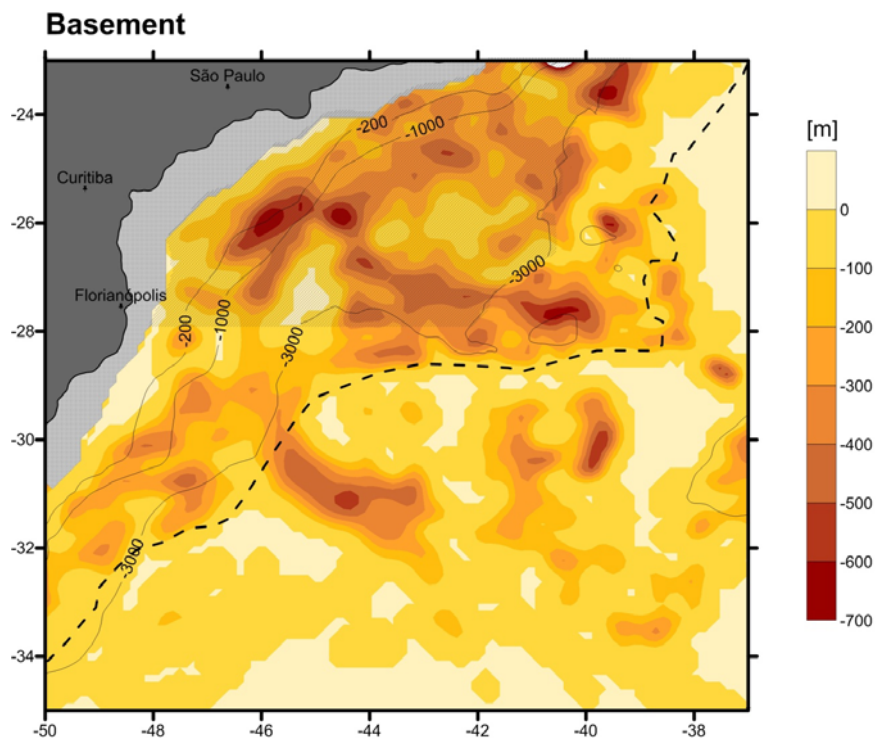


Figure 8 – Topography of gravity basement. The hatched regions (continuous and dotted lines) refer, respectively, to the Santos Basin area and the area where the gravity data are unreliable. The crustal boundary is represented by the dashed line, and the bathymetric contours refer to the depths 200, 1000 and 3000 m.

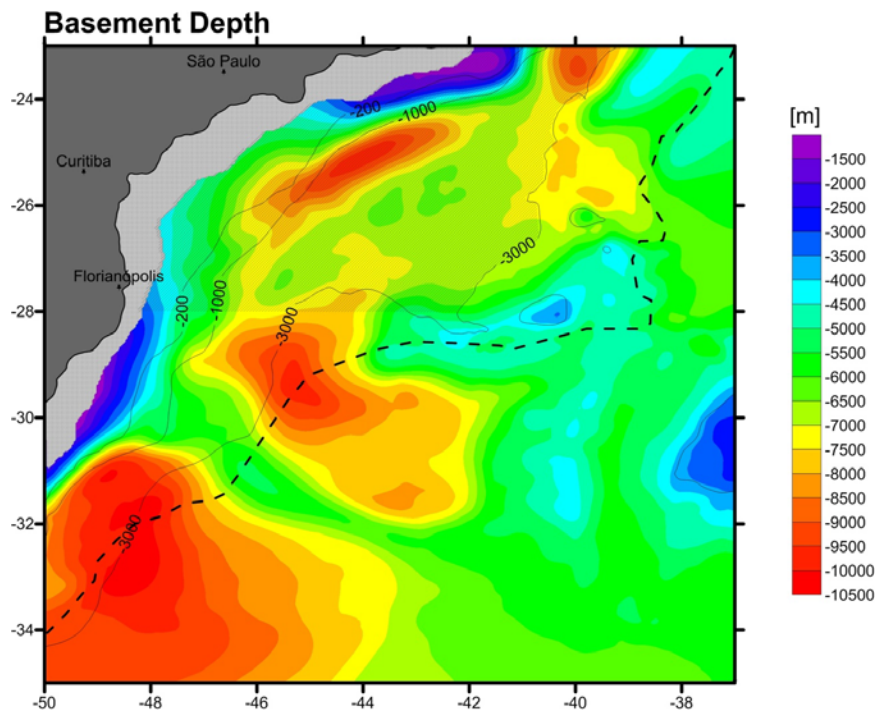


Figure 9 – Basement depth. The hatched regions (continuous and dotted lines) refer, respectively, to the Santos Basin area and the area where the gravity data are unreliable. The crustal boundary is represented by the dashed line, and the bathymetric contours refer to the depths 200, 1000 and 3000 m.

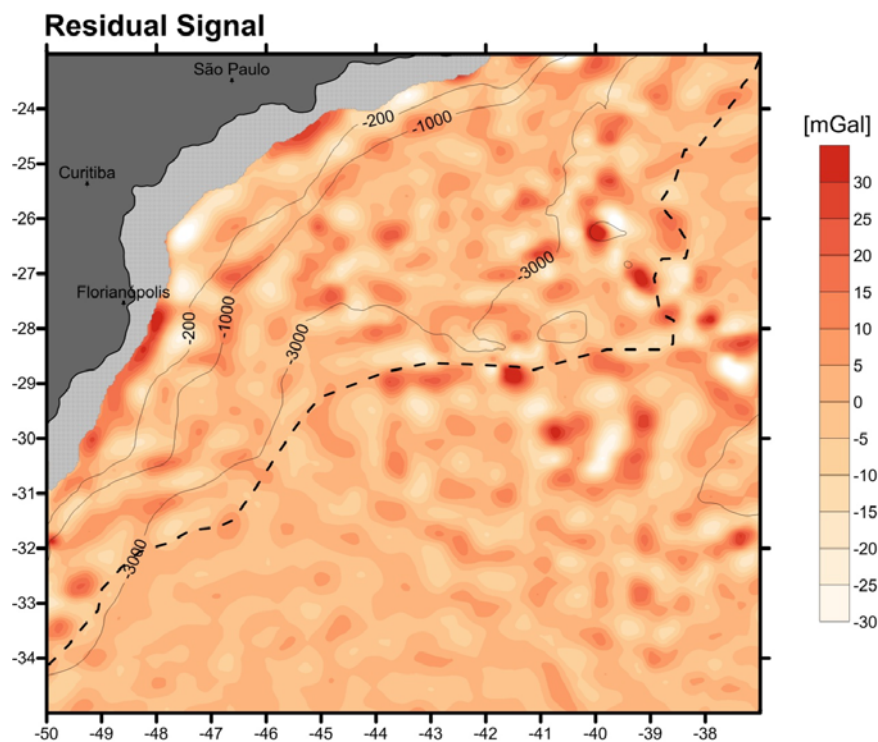


Figure 10 – Difference between the gravity field used as input data and the CMI gravity field. The hatched regions (continuous and dotted lines) refer, respectively, to the Santos Basin area and the area where the gravity data are unreliable. The crustal boundary is represented by the dashed line, and the bathymetric contours refer to the depths 200, 1000 and 3000 m.

represent a flexural CMI deeper than the gravity CMI. The maximum negative difference is 2 km and evident in two areas, one inside and one very close to the basin eastern boundary. The largest positive difference is approximately 3 km, on the southern edge of the basin, near the 3000 m bathymetric contour. The other positive values will not be discussed in this paper since they are close to the area where the data are not reliable.

One possible interpretation for this difference between the CMIs is the presence of short/medium wavelength features that may be present in the gravity anomaly signal and not in the flexural analysis result. This possibility may be discarded for two main reasons: during inversion, the short-wavelength portion was removed and, therefore, should not be generating this difference. Furthermore, it is possible to think that the features that appear in the gravity anomaly data could not appear during the flexural analysis if such features were over a crust region with enough flexural rigidity to support them without deforming. The elastic thickness values were analyzed to verify this second hypothesis (Fig. 11). The circled areas represent the largest differences found between the depth of gravimetric and flexural CMIs.

The map shows that the elastic thickness values in the areas of greatest difference between the CMIs are low, especially between 4 and 6 km, indicating a low flexural rigidity in the region.

This analysis allows to postulate that the differences may have another source, and may be related to the complex geological context in the region, such as the presence of salt domes in the Santos Basin.

The works of Meisling et al. (2001), Izeli (2008), Caldas & Zalán (2009) and Souza et al. (2009) interpreted seismic profiles in the presence of salt domes in the region, allowing to accept the interpretation proposed in this paper as reasonable.

The residual gravity field (Eq. 5) of the basement shows a range of positive anomalies starting at the 3000 m bathymetric contour aligned in the northwest direction (NW). These anomalies were discussed in works such as Demercian (1996) and Meisling et al. (2001).

According to Meisling et al. (2001), these positive gravity anomalies, when analyzed along regional seismic profiles, can be interpreted as coming from volcanic rocks, locally overlapped by thin layers of Aptian evaporites, whose facies are well layered and were interpreted as anhydrites.

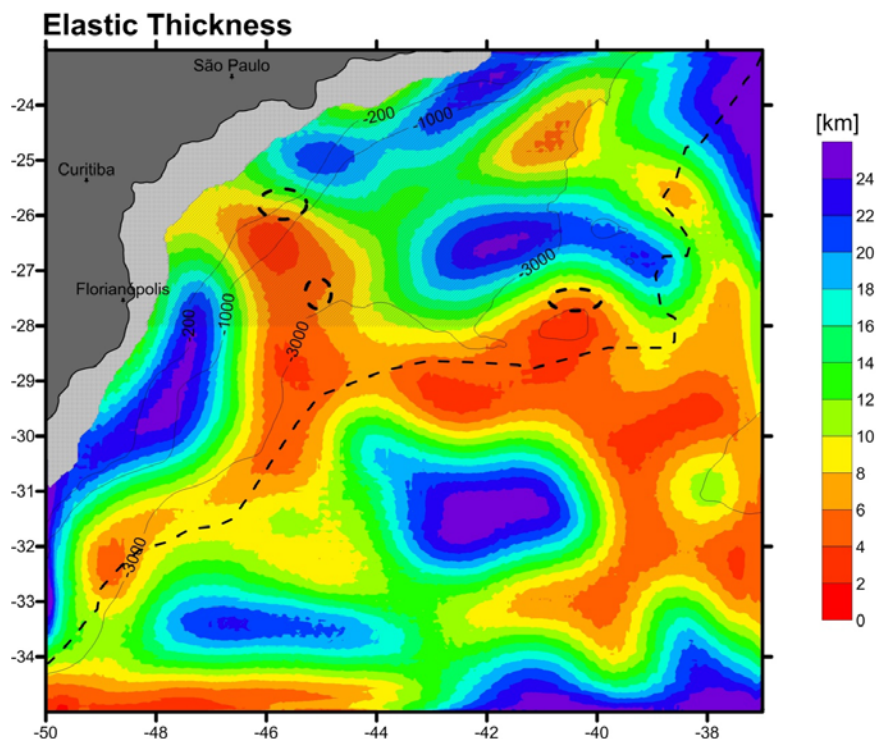


Figure 11 – Elastic Thickness model. The hatched regions (continuous and dotted lines) refer, respectively, to the Santos Basin area and the area where the gravity data are unreliable. The crustal boundary is represented by the dashed line, and the bathymetric contours refer to the depths 200, 1000 and 3000 m.

According to these authors, these anticlines were active volcanic ridges during the deposition of evaporites. Along these ridges, volcanic activity continued during and after the Aptian, mobilizing evaporites and combining them with volcanoclastic deposits. These features were mapped by Demercian (1996) and named as Avedis volcanic chain – a pre-salt high.

The northern portion of the Santos Basin is characterized by large-scale tectonic features with intense diapirism. The processes that generated these features were originated mainly by the uplift of the basement during the Upper Cretaceous in the adjacent portion of the basin. According to Macedo (1989) and Pereira & Macedo (1990), this uplift has induced the progradation of thick coastal sedimentary wedges, creating a large-scale shift in marine sediments toward the São Paulo Plateau, on top of the evaporite layer (Aptian). This shift is accommodated along the Cabo Frio fault.

The basement depth is shown in Figures 8 and 12. The basement structure represented in 3D (Fig. 12) reveals two prominent features. The first is inferred as the possible pre-salt high, discussed above, and the other is a longilineal feature, coincident with the Cabo Frio Fault, with depths reaching approximately

10,500 m between the coordinates (26°S, 46°W) and (24°S, 42°W).

Five basement depth values obtained from wells found between 26°S and 24°S latitudes and 46°W and 44°W longitudes were used to constrain the basement depth. These values were taken from Assine et al. (2008), Cainelli & Mohriak (1999) and ANP (Agência Nacional do Petróleo, Gás Natural e Biocombustíveis – National Petroleum Agency). Table 1 shows basement depth values from wells used as constraints, basement depth values found in this work and their differences.

Table 1 – Well number, basement depth constraint values, basement depth found in this paper and the difference between them.

Well	Basement depth constraints (m)	Basement depth (m)	Difference (m)
SPS-14	5400	5990	590
SPS-20	9200	6775	-2425
SPS-11	8900	7841	-1059
SPS-21	9100	6650	-2450
SPS-05	9300	7310	-1990

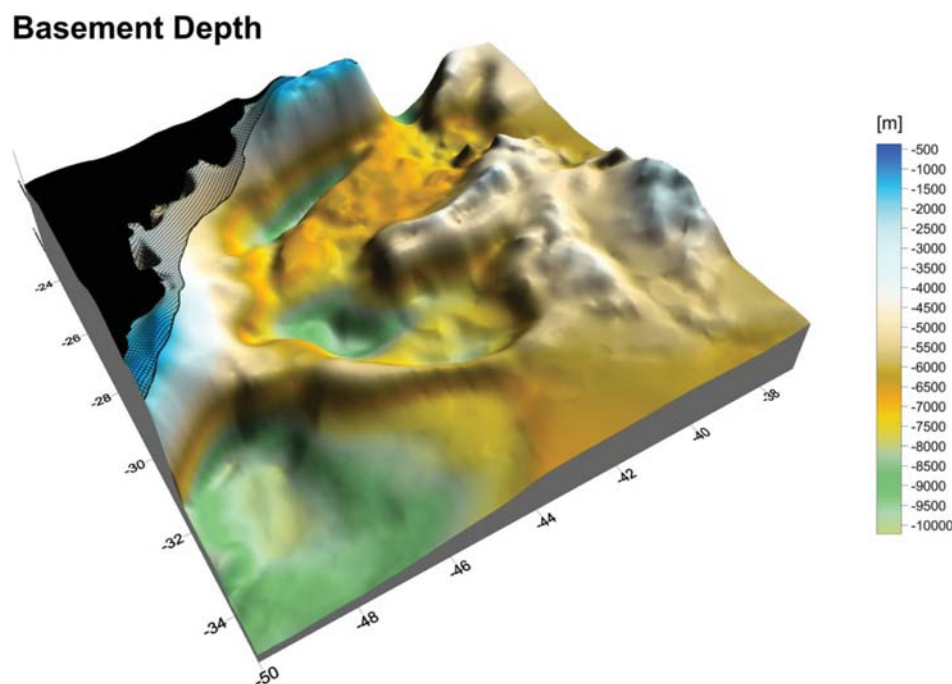


Figure 12 – Perspective representation of the basement depth. The crosshatched region refers to the area where the gravity data are unreliable.

It is noteworthy that the values are quite high in some points. In the case of the basement, a depth difference of about 2 km is crucial for some types of applications. The exception is the first value (well SPS-14) with a difference of 590 m. The basement depth at the location of this well was the only one that was deeper in the model than in the constraint. In all other wells, the basement was shallower in the model than the indicated well values (SPS-05, SPS-11, SPS-20 and SPS-21). A possible explanation for this small difference in the first value may be the penetration of the well SPS-14, which was the only one that almost reached the basement. The penetration of the remaining wells are more than 3 km above the basement, enabling larger errors.

CONCLUSIONS

The basement topography was determined from the analysis of combined gravity data obtained by ship and satellite altimetry, bathymetry data and information on the sediment thickness and the crustal structure of the Santos Basin.

The method proposed in this work to investigate the basement depth is advantageous because it is independent of seismic data. The gravimetric method can be applied quickly, with less environmental impact and fewer costs for acquiring and interpreting the data. In addition, the depth to the basement presented in this paper represents the physical surface below the sedimentary layer, which may be different from the surface pro-

vided by the seismic, which is the deepest observable reflector in the seismic reflection profiles and might not correspond to the sediment base.

The CMI was obtained by gravimetric inversion and seismic refraction data obtained by Leyden et al. (1971) and Zalán et al. (2011) were used to constrain the model. The RMS error found between these data and the model obtained was 1.9 km; however, for best results, additional data could be entered into the model.

The depth to basement values obtained by gravimetric inversion when compared to the values obtained by flexural analysis, showed small differences. The largest differences may be associated with salt diapirs as described in the literature for the Santos Basin (Meisling et al., 2001; Izeli, 2008; Caldas & Zalán, 2009; Souza et al., 2009).

The basement residual gravity field was obtained by subtracting the CMI and sediment gravimetric signal from the observed gravimetric.

The inversion of this residual gravity field resulted in the topography of the basement, revealing a prominent positive feature up to 700 m, which was related to the Avedis volcanic ridge previously recognized by Demercian (1996) and Meisling et al. (2001).

The estimated basement depth ranged from 500 to 10,500 m. The deepest area of the basement is coincident with the Cabo Frio Fault (Macedo, 1989; Pereira & Macedo, 1990; Assine et al., 2008; Zalán et al., 2009).

The Santos Basin basement description in this study is unprecedented in the literature. In addition to this work, the methodology has already been tested in the South China Sea, and its application was successful in both cases. The method proved to be reliable and can be applied in other marginal basins aiding hydrocarbon exploration.

REFERENCES

- ASSINE ML, CORRÊA FS & CHANG HK. 2008. Migração de depocentros na Bacia de Santos: importância na exploração de hidrocarbonetos. *Revista Brasileira de Geociências*, 38(Suppl. 2): 111–127.
- BLAKELY RJ. 1995. *Potential Theory in Gravity and Magnetic Applications*. Cambridge Univ. Press, 441 pp.
- BRAITENBERG C & ZADRO M. 1999. Iterative 3D gravity inversion with integration of seismologic data. *Bollettino Di Geofisica Teorica ed Applicata*, 40(3-4): 469–475.
- BRAITENBERG C, EBBING J & GÖTZE H-J. 2002. Inverse modelling of elastic thickness by convolution method: The Eastern Alps as a case example. *Earth Planet. Sci. Lett.*, 202: 387–404.
- BRAITENBERG C, WANG Y, FANG J & HSU HT. 2003. Spatial variations of flexure parameters over the Tibet-Quinghai plateau. *Earth Planet. Sci. Lett.*, 205(3-4): 211–224.
- BRAITENBERG C, WIENECKE S & WANG Y. 2006. Basement structures from satellite-derived gravity field: South China Sea ridge. *J. Geophys. Res.*, 111: B05407, doi: 10.1029/2005JB003938.
- BRAITENBERG C, WIENECKE S, EBBING J, BORN W & REDFIELD T. 2007. Joint Gravity and Isostatic Analysis for Basement Studies – A Novel Tool. In: *EGM 2007 International Workshop, Innovation in EM, Grav and Mag Methods: a new Perspective for Exploration*. Extended Abstracts, Villa Orlandi, Capri – Italy, pp. 15–18.
- CAINELLI C & MOHRIAK WU. 1999. Some remarks on the evolution of sedimentary basins along the Eastern Brazilian continental margin. *Episodes*, 22(3): 206–216.
- CALDAS MF & ZALÁN PV. 2009. Reconstituição cinemática e tectono-sedimentação associada a domos salinos nas águas profundas da Bacia de Santos, Brasil. *Boletim de Geociências da Petrobras*, 17(2): 227–248.
- CALMANT S & BAUDRY N. 1996. Modelling bathymetry by inverting satellite altimetry data: A review. *Mar. Geophys. Res.*, 18: 123–134.
- DEMERCIAN LS. 1996. A halocinese na evolução do Sul da Bacia de Santos do Aptiano ao Cretáceo Superior. Master's thesis, Universidade Federal do Rio Grande do Sul, Porto Alegre, Brazil, 201 pp.
- DIVINS DL. 2003. Total Sediment Thickness of the World's Oceans & Marginal Seas. NOAA National Geophysical Data Center, Boulder, CO.
- EBBING J, BRAITENBERG C & GÖTZE H-J. 2006. The lithospheric density structure of the Eastern Alps. *Tectonophysics*, 414: 145–155.
- GEBCO. 2010. The GEBCO One Minute Grid, version 2.0, Available on: <<http://www.gebco.net>>. Access on: March 14th, 2010.
- HWANG C. 1999. A bathymetric model for the South China Sea from Satellite altimetry and depth data. *Mar. Geod.*, 22: 37–51.
- IZELI MGB. 2008. Controle estrutural do embasamento emerso na porção central da Bacia de Santos, utilizando sensoriamento remoto e interpretação sísmica. Final Graduation Paper on Geology, Instituto de Geociências e Ciências Exatas – UNESP, Rio Claro, Brazil, 65 pp.
- KARNER GD & WATTS AB. 1982. On isostasy at Atlantic-Type Continental Margins. *J. Geophys. Res.*, 87(B4): 2923–2948.
- KUMAR RTR, MAJU TK, KANDPAL SC, SENGUPTA D & NAIR RR. 2011. Elastic Thickness estimates at northeast passive margin of North America and its implications. *J. Earth Syst.*, 120(3): 447–458.
- LEYDEN R, LUDWIG WJ & EWING J. 1971. Structure of the continental margin of Punta del Este, Uruguay, and Rio de Janeiro, Brazil. *AAPG Bulletin*, 55: 2161–2173.
- MACEDO JM. 1989. Evolução tectônica da Bacia de Santos e áreas continentais adjacentes. *Boletim de Geociências da Petrobras*, 3: 159–173.
- MEISLING KE, COBBOLD PR & MOUNT VS. 2001. Segmentation of an obliquely rifted margin, Campos and Santos basins, southeastern Brazil. *AAPG Bull.*, 85(11): 1903–1924.
- MIO E. 2005. Modelagem crustal da Bacia de Santos pela integração de métodos geofísicos. Master dissertation, Instituto de Geociências, Universidade Estadual Paulista, Rio Claro, Brazil. 94 pp.
- MIO E, CHANG HK & CORRÊA FS. 2005. Integração de métodos geofísicos na modelagem crustal da Bacia de Santos. *Brazilian Journal of Geophysics*, 23(3): 275–284.
- MOLINA EC. 2009. O uso de dados de missões geodésicas de altimetria por satélite e gravimetria marinha para a representação dos elementos do campo de gravidade terrestre. Tese de livre docência, Departamento de Geofísica, IAG-USP, Universidade de São Paulo, São Paulo, Brazil, 100 pp.
- MOREIRA JLP, MADEIRA CV, GIL JA & MACHADO MAP. 2007. Bacia de Santos. *Boletim de Geociências da Petrobras*, 15(2): 531–549.
- PARKER RL. 1972. The rapid calculation of potential anomalies. *Geophys. J. R. Astr. Soc.*, 31: 447–455.
- PEREIRA MJ & MACEDO JM. 1990. A Bacia de Santos: perspectivas de uma nova província petrolífera na plataforma continental sudeste brasileira. *Boletim de Geociências da Petrobras*, 4: 3–11.
- RAMILLIEN G & CAZENAVE A. 1996. Global bathymetry derived from altimeter data of the ERS-1 geodetic mission. *J. Geodyn.*, 23(2): 129–149.

- RUSSO RM & SPEED RC. 1994. Spectral analysis of gravity anomalies and the architecture of tectonic wedging, NE Venezuela and Trinidad. *Tectonics*, 13(2): 613–622.
- SANDWELL DT & SMITH WHF. 2001. Bathymetric estimation. In: FU L-L & CAZENAIVE A (Eds.). *Satellite Altimetry and Earth Sciences*. Elsevier, New York. pp. 441–457.
- SCLATER JG & CHRISTIE PAF. 1980. Continental stretching: An explanation of the Post-Mid-Cretaceous subsidence of the central North Sea basin. *J. Geophys. Res.*, 85: 3711–3739.
- SMITH WHF & SANDWELL DT. 1997. Global sea floor topography from satellite altimetry and ship depth soundings. *Science*, 277: 1956–1962.
- SOUZA IA, EBERT HD, CASTRO JC, SOARES JR AV, SILVA GHT & BENVENUTTI CF. 2009. Caracterização das falhas de transferência na porção norte da Bacia de Santos a partir da integração de dados geológicos e geofísicos. *Boletim de Geociências da Petrobras*, 17(1): 109–132.
- SUPKO PR, PERCH-NIELSEN K & CARLSON RL. 1997. Introduction and explanatory notes, Leg 39, Deep Sea Drilling Project. DSDP Volume XXXIX, doi: 10.2973/dsdp.proc.39.
- TASSARA A, SWAIN C, HACKNEY R & KIRBY J. 2007. Elastic thickness structure of South America estimated using wavelets and satellite-derived gravity data. *Earth Planet. Sci. Lett.*, 253: 17–36.
- TURCOTTE DL & SCHUBERT L. 1982. *Applications of Continuum Physics to Geological Problems*. John Wiley and Sons, New York, 450 pp.
- WATTS AB. 2001. *Isostasy and Flexure of the Lithosphere*. Cambridge University Press, Cambridge, 458 pp.
- WIENECKE S. 2006. A new analytical solution for the calculation of flexural rigidity: significance and applications. PhD thesis, Freie Universität Berlin, Berlin, Germany, Available on: <<http://www.diss.fu-berlin.de/2006/42>>. Access on: April 17th, 2010.
- WOODWARD D & WOOD R. 2000. Bathymetry sediment thickness and crustal structure from satellite gravity data. *Exploration Geophysics*, 31(2): 89–93, doi: 10.1071/EG00089.
- ZALÁN PV, SEVERINO MCG, RIGOTI CA, MAGNAVITA LP, OLIVEIRA JAB & VIANNA AR. 2011. An entirely new 3D-view of the crustal and mantle structure of a South Atlantic passive margin – Santos, Campos and Espírito Santo Basins, Brazil. In: AAPG Annual Convention, Houston TX, USA, Extended Abstracts, Search and Discovery, article #30177.

Recebido em 3 maio, 2012 / Aceito em 4 março, 2015
 Received on May 3, 2012 / Accepted on March 4, 2015

NOTES ABOUT THE AUTHORS

Renata Constantino. Graduated in Oceanography, focusing on analysis and satellite image processing in the South Atlantic region. Specialist in science communication from ECA/ABRADIC – USP. Masters in Geophysics from IAG/USP, focusing on interpretation of gravity anomalies in the Santos Basin. Currently, pursuing a PhD in Geophysics from IAG/USP, focusing on interpretation of seismic and gravity data in the Santos Basin and modeling of pre-salt layer.

Eder Cassola Molina. Graduated in Geophysics from IAG-USP, and in Chemical Engineering from FEI. Holds a master's degree, doctorate and full professorship in Geophysics from USP. Currently, works as a Professor at IAG-USP, undergraduate and graduate, since 1988. Works in the fields of gravimetry, geomagnetism and development of numerical methods to process geophysical data.